Proceedings of the ASME 2010 10th Biennial Conference on Engineering Systems Design and Analysis
ESDA2010
July 12-14, 2010, Istanbul, Turkey

ESDA2010-25136

A Numerical Study on Flow Characteristics of 2D Vertical Liquid Jet Striking a Horizontal Surface

M. Kimiaghalam
Department of Mechanical Engineering
Ferdowsi University of Mashhad
Mashhad, Iran
Email: mo_ki39@um.ac.ir

M. Passandideh-Fard
Associate Professor
Department of Mechanical Engineering
Ferdowsi University of Mashhad
Mashhad, Iran
Email: mpfard@um.ac.ir

ABSTRACT

We studied numerically impingement of vertical liquid jets of moderate Reynolds number for both Newtonian and non-Newtonian liquids to clarify the structure formation of circular hydraulic jump and the phenomenon of jet buckling. First, we have studied the hydraulic jump characteristics and governing parameters for a laminar water jet. Moreover, different types of hydraulic jump have been investigated by varying the height of a circular wall around the bed in flow downstream. The results show that a circular hydraulic jump has two kinds of steady states which can be reached by changing wall height. Next, we studied the impingement of a non-Newtonian liquid jet on a solid surface. In this case, we observe that instead of having a significant hydraulic jump, jet buckling phenomenon happens. The results were used in order to achieve a better understanding of the jet buckling phenomenon and the conditions in which this phenomenon happens.

NOMENCLATURE

D	jet inlet diameter
H	jet length
R_j	jump radius
a	jet diameter at the point of impingement
d or H_∞	outer depth
Q	inlet volume flux
ΔH	jump height
u	inlet velocity
ρ	liquid density
η	liquid viscosity

INTRODUCTION

When a vertical Newtonian liquid jet impinges on a horizontal surface and spreads out radially on the surface a circular hydraulic jump is formed. At the hydraulic jump, the height of the liquid surface suddenly varies and the flow also changes from a rapid (supercritical) flow to a slow (subcritical) flow. A picture of the circular hydraulic jump is shown in Fig. 1.

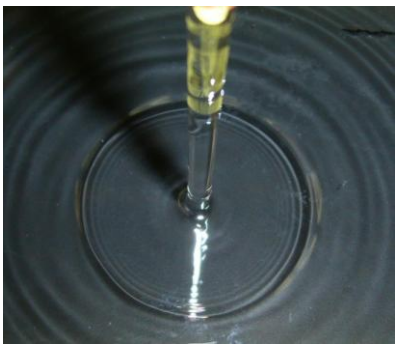

Figure 1. PICTURE OF A STATIANARY CIRCULAR HYDRAULIC JUMP [28]

The circular hydraulic jump is common in daily life and appears to be a simple phenomenon. However, it is much more complicated than it seems to be. In fact, it involves a strongly distorted free surface, a boundary layer and separation of flow. Studies concerning this phenomenon have been done by various approaches [1–12]. The circular hydraulic jump is relatively easily created in laboratory experiments, while the theoretical and numerical studies are limited by the complexities mentioned above. Especially when we use water as the liquid, these complexities will arise because of the turbulent effects of water. The experimental results show that a circular hydraulic jump has two kinds of steady states which can be reached by changing the height of a circular wall (d) around the bed in flow downstream. When d is low or 0, a type I jump is formed as shown in Fig. 2(a). A type I jump contains an eddy on the bottom, called a 'separation bubble'. On increasing d, the jump becomes steeper until d reaches the critical dc. If d becomes larger than dc, the liquid outside of the jump topples and another steady state, a type II jump, is formed as shown in Fig. 2(b) and 2(c). An eddy under the surface in a type II jump, the secondary circulation, which is usually called a 'roller', is observed. The existence of a roller distinguishes the two types of jumps.

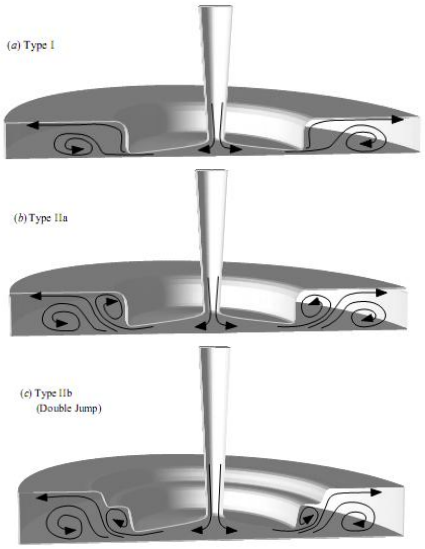

Figure 2. A SCHEMATIC ILLUSTRATION OF THE PROGRESSION IN FLOW STRUCTURE OF THE CIRCULAR LAMINAR HYDRAULIC JUMP PROMPTED BY INCREASING THE OUTER DEPTH. THE STEADY SYMMETRY-BREAKING INSTABILITIES EMERGE EXCLUSIVELY FROM THE TYPE ii JUMPS. [27]

A simple and common theoretical approach to inviscid hydraulic jump problems is due to Rayleigh [1]. In this approach, hydraulic jumps are regarded as a shock, a discontinuity, based on the analogy between the shallow water theory and gas theory [13]. Thus flow structure in the jump region is neglected. This approach has been widely used in hydraulic engineering. In a theoretical study of circular hydraulic jumps, a scaling relation of the radius of the circular hydraulic jump has been proposed [6]. This scaling relation is simple but agrees rather well with experimental data. A theoretical model for a type I jump has been developed by Bohr and coworkers [8, 9, 12], but no model for the type II jump is available yet. In the theoretical model of Bohr et al., it is assumed that the pressure distribution is hydrostatic and that the surface tension force is negligible. However, those effects seem to play a crucial role in the formation of hydraulic jumps, especially in the type II state. Numerical simulations have been also performed for the circular hydraulic jump problems in [7], where a preset fixed boundary was used to represent the real free surface of the liquid. It should be noted that direct computation of the free surface of the liquid, which usually appears to be a very difficult problem, is important and essential to a numerical simulation of hydraulic jumps.

When a vertical non-Newtonian liquid jet with a Reynolds number less than a specific value impinges on a horizontal surface, the phenomenon of jet buckling happens. This means that there would be some instability to the liquid jet. In industries like food, chemistry, medical, among others, the phenomenon of jet buckling has a large relevance in tasks involving the filling of containers with liquid like substances. This flow instability is related to the occurrence of some problems like splashing, sloshing and void formation [14-15] and therefore is undesirable. Despite its obvious importance, the literature on this subject is scarce .The jet buckling phenomenon has been studied since the late fifties, when the work entitled "Liquid rope coiling" by Barnes and Woodcock [16] led the way to several experiment al studies, that have been performed until the present time [17-21]. Concerning the theoretical understanding of this phenomenon, the work of Taylor [22] was the pioneer. He noticed that the jet buckling was similar to the buckling instability that occurs in slender beams and concluded that this phenomenon was related to longitudinal compressive stresses in the 'liquid rope'. Zak [23], based in the investigations performed by Cruickshank [4], studied this problem with analytical models and established criteria for the onset of this instability. In the review performed by Bejan [19], in contradiction with the Cruickshank studies [17], it was concluded that this phenomenon can also occur for high Reynolds numbers. Later, Mahadevan et al. [24] showed that the buckling instabilities are an outcome from a competition between compression and bending stresses in slender objects. More recently, Ribe [25] proved that there are other variables involved and demonstrated theoretically that coiling can appear in three distinct dynamical regimes: viscous, gravitational and inertial. The experiment al observance of these three regimes was afterwards performed by Maleki et al. [21]

MATHEMATICAL MODEL

Hydraulic Jump for Newtonian Liquid

For all flows, Fluent solves conservation equations for mass and momentum. For flows involving heat transfer or compressibility, an additional equation for energy conservation is solved. For flows involving species mixing or reactions, species conservation equation are solved or, if the non-premixed combustion model is used conservation equations for the mixture fraction and its variance are solved. Additional transport equations are also solved when the flow is turbulent. In this paper conservation equations for laminar flow are presented.

The Continuity Equation

The tracking of the interface(s) between the phases is accomplished by the solution of a continuity equation for the volume fraction of one (or more) of the phases. For the q^{th} phase, this equation has the following form:

$$\frac{1}{\rho_q}\left[\frac{\partial}{\partial t}\left(\alpha_q\rho_q\right)+\nabla.\left(\alpha_q\rho_q\bar{v}_q\right)=S_{\alpha_q}+\sum_{p=1}^{n}\left(\dot{m}_{pq}-\dot{m}_{qp}\right)\right] \quad (1)$$

Where $\dot{m}_{pq}$ is the mass transfer from phase q to phase p and $\dot{m}_{qp}$ is the mass transfer from phase p to phase q. By default, the source term on the right-hand side of Equation $1, S_{\alpha_q}$, is zero, but we can specify a constant or user-defined mass source for each phase. The volume fraction equation will not be solved for the primary phase; the primary-phase volume fraction will be computed based on the following constraint:

$$\sum_{q=1}^{n}\alpha_q=1 \quad (2)$$

Momentum Conservation Equations

Conservation of momentum in an inertial reference frame is described by

$$\frac{\partial}{\partial t}\left(\rho\bar{V}\right)+\nabla.\left(\rho\bar{V}\bar{V}\right)=-\nabla p+\nabla.\left(\bar{\tau}\right)+\rho\bar{g}+\bar{F} \quad (3)$$

Where p is the static pressure, $\bar{\tau}$ is the stress tensor (described below), and $\rho\bar{g}$ and $\bar{F}$ are gravitational body force and external body forces respectively.

The stress tensor $\bar{\tau}$ is given by

$$\bar{\tau}=\mu\left[\left(\nabla\bar{V}+\nabla\bar{V}^{T}\right)-\frac{2}{3}\nabla.\bar{V}I\right] \quad (4)$$

Where μ is the molecular viscosity, I is the unit tensor, and the second term on the right hand side is the effect of volume dilation.

The mesh used to solve this model was constructed by using Gambit 2.3.16 (FLUENT 6.3.26). The generated mesh contains quadrilateral elements and is shown in Figure 5.

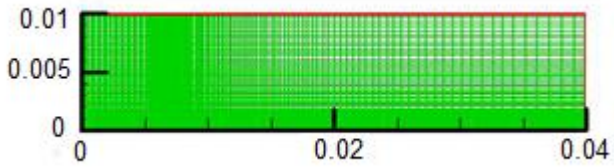

Figure 3. AXISYMETRIC MESH GENERATION

The number of cells per jet radius is 30 CPR and the number of total cells in the Figure 5 is 8500.

Jet Buckling for Non-Newtonian Liquids

To study the phenomenon of jet buckling, in addition to equations mentioned above we have to solve the power law equation as follows.

Viscosity for Non-Newtonian Fluids

For incompressible Newtonian fluids, the shear stress is proportional to the rate-of-deformation tensor $\bar{\bar{D}}$:

$$\bar{\bar{\tau}}=\mu\bar{\bar{D}} \quad (5)$$

where $\bar{\bar{D}}$ is defined by

$$\bar{\bar{D}}=\left(\frac{\partial u_j}{\partial x_i}+\frac{\partial u_i}{\partial x_j}\right) \quad (6)$$

and μ is the viscosity, which is independent of $\bar{\bar{D}}$.

For some non-Newtonian fluids, the shear stress can similarly be written in terms of a non-Newtonian viscosity η:

$$\bar{\bar{\tau}} = \eta(\bar{\bar{D}})\bar{\bar{D}} \qquad (7)$$

In general, η is a function of all three invariants of the rate-of-deformation tensor $\bar{\bar{D}}$. However, in the non-Newtonian models available in FLUENT, η is considered to be a function of the shear rate $\dot{\gamma}$ only. $\dot{\gamma}$ is related to the second invariant of $\bar{\bar{D}}$ and is defined as

$$\dot{\gamma} = \sqrt{\frac{1}{2}\bar{\bar{D}} : \bar{\bar{D}}} \qquad (8)$$

FLUENT provides four options for modeling non-Newtonian flows:

Power law
Carreau model for pseudo-plastics
Cross model
Herschel-Bulkley model for Bingham plastics

Note that the non-Newtonian power law described below is used in this study.

Non-Newtonian flow will be modeled according to the following power law for the non-Newtonian viscosity:

$$\eta = k\dot{\gamma}^{n-1}e^{T_0/T} \qquad (9)$$

FLUENT allows you to place upper and lower limits on the power law function, yielding the following equation:

$$\eta_{\min} < \eta = k\dot{\gamma}^{n-1}e^{T_0/T} < \eta_{\max} \qquad (10)$$

where k, n, T_o, $\eta_{\min}$, and $\eta_{\max}$ are input parameters. k is a measure of the average viscosity of the fluid (the consistency index); n is a measure of the deviation of the fluid from Newtonian (the power-law index), as described below; T_o is the reference temperature; and $\eta_{\min}$ and $\eta_{\max}$ are, respectively, the lower and upper limits of the power law. If the viscosity computed from the power law is less than $\eta_{\min}$, the value of $\eta_{\min}$ will be used instead. Similarly, if the computed viscosity is greater than $\eta_{\max}$, the value of $\eta_{\max}$ will be used instead. The value of n determines the class of the fluid:

n = 1 $\rightarrow$ Newtonian Fluid
n = 2 $\rightarrow$ shear-thickening (dilatants fluids)
n = 3 $\rightarrow$ shear-thinning (pseudo-plastics)

In this case, the number of cells per inlet jet radius is 30 CPR and number of total cells is 13500. The generated mesh contains quadrilateral elements and is shown in Figure 7.

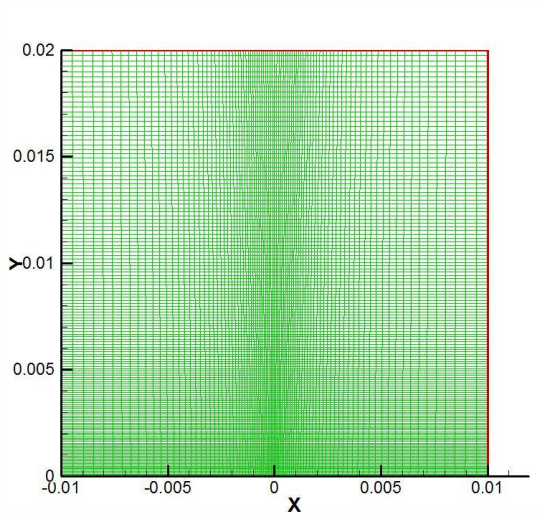

Figure 4. 2D MESH GENERATION

RESULTS

We have used a simple 2D Axisymetric geometry, shown in Fig. 5 for the impingement of a Newtonian liquid jet. At inlet the velocity is 0.3 m/s (Re=3000) and the operating pressure is 101325 Pascal. We have studied the effect of outer depth by changing the height of the circular wall shown in Fig.5.

Figure 5.GEOMETRY EMPLOYED TO STUDY THE STRUCTURE FORMATION OF CIRCULAR HYDRAULIC JUMPS. IN THIS CASE d=1mm

Flow properties of the Newtonian liquid are given in table 1. We have used water properties in this case.

Table 1. NEWTONIAN LIQUID PROPERTIES

Density (Kg/m^3)	998.2
Viscosity (Kg/m-s)	0.001

In the study of the impingement of a Non-Newtonian liquid jet we have used a 2D geometry. Fig. 6 shows the geometry employed to study the phenomenon of jet buckling.

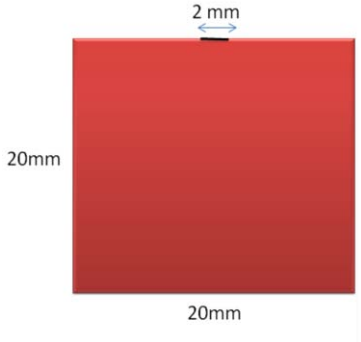

Figure 6. GEOMETRY EMPLOYED TO STUDY THE STRUCTURE FORMATION OF JET BUCKLING

The flow properties of the Non-Newtonian liquid are shown in table 2.

Table 2. NON-NEWTONIAN LIQUID PROPERTIES AND POWER LAW PARAMETERS

Density (Kg/m^3)	1360
Power law index (n)	0.4851
Consistency index k (kg.s^n-2/m)	0.2073
Reference temperature (°K)	310
Minimum viscosity limit Π_{max}(kg/m-s)	30
Maximum viscosity limit Π_{min}(kg/m-s)	20

Validation

The present numerical scheme on the hydraulic jump has been compared with the results of Bush & Aristoff [26] which is a correction to the Watsons model by considering the effect of surface tension. The comparison is shown in Fig. 7. Regarding Fig. 7, it can be observed that our numerical results are in a good agreement with results presented by Bush & Aristoff [26]. For the case of jet buckling we have compared our results with the results of Cruikshank and Munson [17] and they are in a good agreement as it will be shown later in this paper.

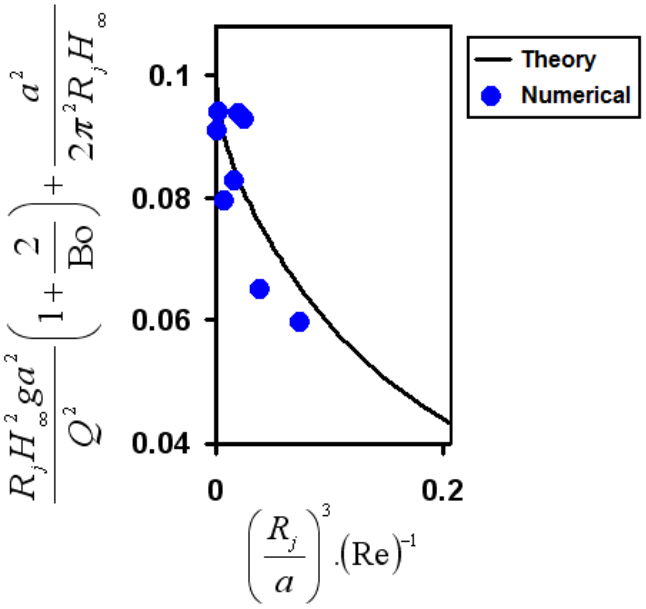

Figure 7. COMPARISON OF PRESENT NUMERICAL STUDY WITH BUSH & ARISTOFF RESULTS FOR THE DEPENDENCE OF JUMP RADIUS R_j ON THE GOVERNING PARAMETERS, WHERE a IS THE JET RADIUS AT THE POINT OF IMPINGEMENT, H_∞ IS THE OUTER DEPTH, AND $B_o=\rho g R_j \Delta H/\sigma$ IS THE JUMP BOND NUMBER.

Circular Hydraulic jump results

Figures 8 through 11 show the effect of inlet volume flux, liquid viscosity, and outer depth on the jump radius.

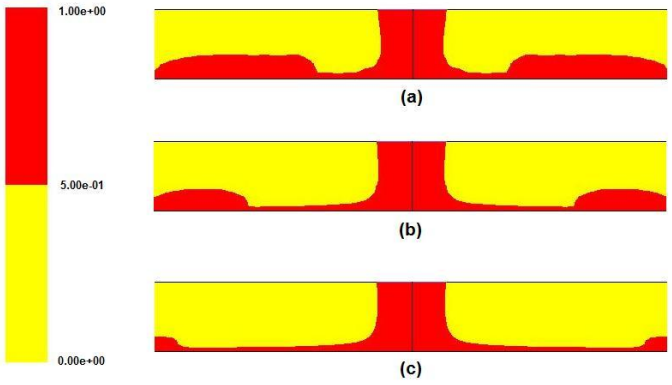

Figure 8. EFFECT OF JET INLET VOLUME FLUX ON THE JUMP RADIUS (a) Q=2.355e-05 m^3/s (b) Q=3.14e-05 m^3/s (c) Q=3.92.5e-05 m^3/s

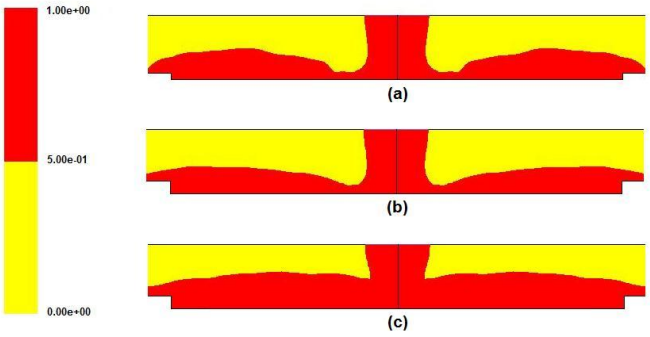

Figure 9. EFFECT OF OUTER DEPTH ON THE JUMP RADIUS (a) d=1mm (b) d=2mm (c) d=3mm

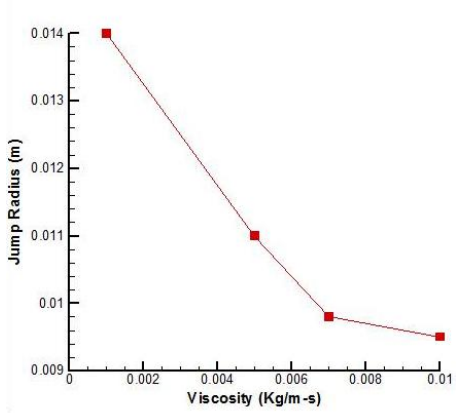

Figure 10. JUUMP RADIUS VERSUS THE LIQUID VISCOSITY

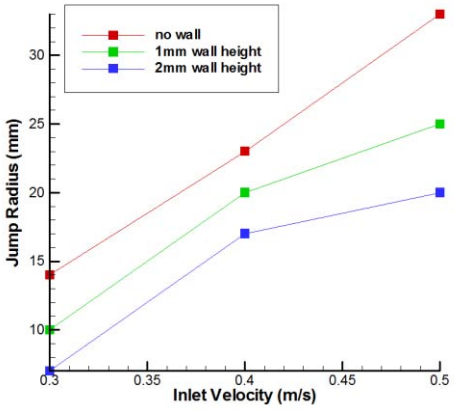

Figure 11. JUMP RADIUS VERSUS THE INLET VELOCITY AND DOWNSTREAM HEIGHT.

Regarding Figures 8 through 11, it can be concluded that the jump radius will increase when the inlet volume flux increases and it will decrease when liquid viscosity or outer depth increases.

Furthermore, we have studied the effect of outer depth on flow vortexes and the transition from type I jump to type II.
Regarding Fig. 12, the case of Fig. 12(a) shows a type I jump which contains an eddy on the bottom, called a 'separation bubble'. In the case of Fig. 12(b) we have a type II jump with an eddy under the surface and a secondary circulation, called a 'roller'. In Fig. 12(c) again we have a type II jump and in the Fig. 12(d) due to the extension in the roller no jump will occur.
It can be seen that the transition will occur for an outer depth between 0 and 1 mm. studying several cases with outer depths in this range, it has been investigated that the transition will occur for d/D of 0.06 where d is the outer depth and D is the jump diameter.

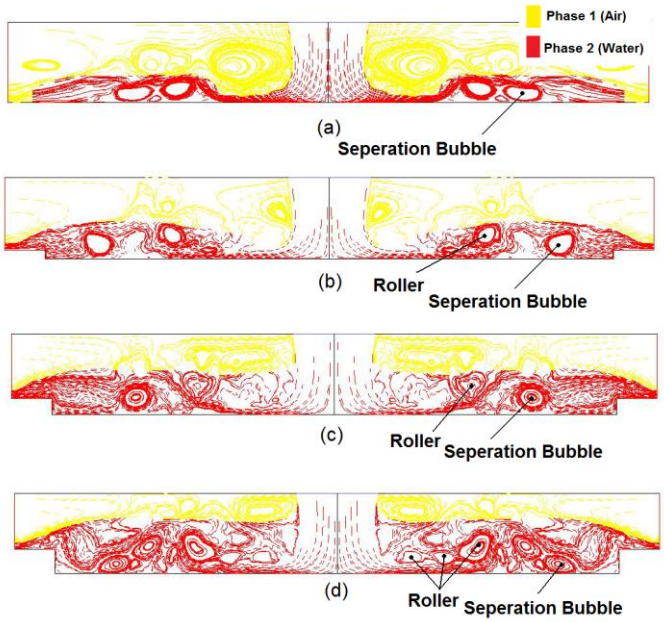

Figure 12. EFFECT OF OUTER DEPTH ON FLOW VORTEXES AND JUMP TYPE (a) d=0mm, (b) d=1mm, (c) d=2mm, (d) d=3mm

Jet Buckling Results

In Fig. 13 a schematic illustration for the phenomenon of jet buckling in a series of time steps is shown. Due to this Figure, it is obvious that the structure formation for the impingement of a Non-Newtonian liquid on a horizontal surface is clearly different from one of a Newtonian liquid.
In this case as the liquid viscosity is so high, it cannot spread on the surface and as a result, by continuance in the jet flow there would be some instability to the liquid jet and the jet buckles.

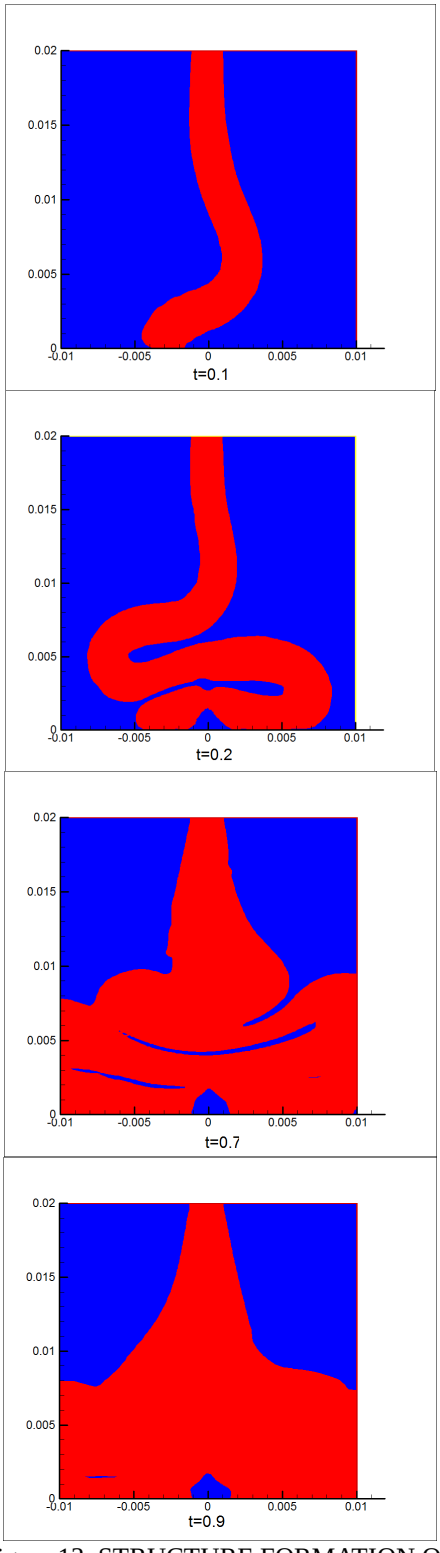

Figure 13. STRUCTURE FORMATION OF JET BUCKLING (NUMERICAL RUN 1)

During the numerical study several different conditions were tested and some of them are listed in Table 3.

Table 3.
NUMERICAL CONDITIONS EMPLOYED IN THE STUDY OF JET BUCKLING

Numerical Run	Inlet Velocity (m/s)	Reynolds ($\rho ud/\eta_{max}$)	H/D	Flow Regime
1	2.4	0.217	10	Jet Buckling
2	8	0.725	10	Transition
3	13.5	1.225	10	Smooth Filling
4	2.4	0.217	5	Smooth Filling
5	2.4	0.217	7.2	Transition
6	2.4	0.217	12.5	Jet Buckling

Results show that the occurrence of jet buckling depends on the Reynolds number and H/D where H is the jet length and D is the jet inlet diameter. Regarding table 1, we can investigate the conditions in which the phenomenon of jet buckling happens. In a rather good agreement with observations published by Cruikshank and Munson [17] it can be seen that a Non-Newtonian liquid jet buckles if both conditions Re < 0.725 and H/D >7.2 are satisfied.

When a Non-Newtonian liquid impinges on a horizontal surface (in no-slip condition) the shear rate will increase at the point of impingement as a result of increase in velocity gradients. This increase in the shear rate will result in reduction of liquid viscosity (Fig. 14). The relatively significant difference in viscosity of different layers results in the deformation of liquid jet and the phenomenon of jet buckling. It is worth mentioning that jet buckling is a physical instability and it lasts just for a short time and after a while there would be no buckling and the liquid would be in physical stability.

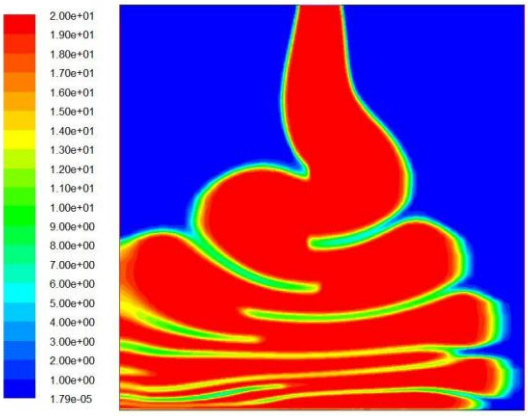

Figure 14. CONTOURS OF VISCOSITY (Kg/m-s) FOR A NON-NEWTONIAN LIQUID JET

CONCLUSION

The impingement of vertical Newtonian and non-Newtonian liquid jets has been studied numerically to clarify the structure formation of circular hydraulic jump and the phenomenon of jet buckling. With regard to the results and points made above it can be concluded that in the case of circular hydraulic jump, the jump radius will increase when the inlet volume flux increases and it will decrease when liquid viscosity or outer depth increases. Furthermore, it has been investigated that the transition from a type 1 jump to a type 2 will occur for d/D of 0.06. In the case of jet buckling phenomenon, it can be seen that a Non-Newtonian liquid jet buckles if both conditions Re < 0.725 and H/D >7.2 are satisfied.

REFRENCES

[1] L. Rayleigh, Proc. Roy. Soc. London A 90 (1914) 324.

[2] I. Tani, J. Phys. Soc. Jpn. 4 (1949) 212.

[3] V.T. Chow, Open Channel Hydraulic, McGraw-Hill, New-York, 1959

[4] E.J. Watson, J. Fluid Mech. 20 (1964) 481.

[5] A.D.D. Craik, R.C. Latham, M.J. Fawkes, P.W.F. Gribbon, J.Fluid Mech. 112 (1981) 347.

[6] T. Bohr, P. Dimon, V. Putkaradze, J. Fluid Mech. 254 (1993), 635.

[7] T. Bohr, C. Ellegaard, A.E. Hansen, A. Haaning, Physica B 228 (1996) 1.

[8] T. Bohr, V. Putkaradze, S. Watanabe, Phys. Rev. Lett. 79 (1997) 1038.

[9] V. Putkaradze, Ph.D. Thesis, Niels Bohr Institute, University of Copenhagen, 1997.

[10] K . Yokoi, F. Xiao, Phys. Lett. A 257 (1999) 153.

[11] K. Yokoi, F. Xiao, Phys. Rev. E 61 (2000) R1016.

[12] S. Watanabe, V. Putkaradze, T. Bohr, Preprint, physics/0008219 (2000).

[13] L.D. Landau, E.M. Lifshitz, Fluid Dynamics, Pergamon Press, Oxford, 1987.

[14] Tome, M.F., et al., An experimental and numerical investigation of container filling with viscous liquids. International Journal for Numerical Methods in Fluids, 1999. 31(8): pp. 1333-1353.

[15] Gomon, M., Experimental Study of Highly Viscous Impinging Jets. 1998, Department of Mechanical Engineering, The University of Texas.

[16] Barnes, G. and R. Woodcock, Liquid rope-coil effect. Am. J. Phys., 1958. 26: pp. 205–209.

[17] Cruickshank, J.O. And B.R. Munson, Viscous-Fluid Buckling of Plane and Axisymetric Jets. Journal of Fluid Mechanics, 1981. 113(DEC): pp. 221-239.

[18] A. Bejan, Experiments on the Buckling of Thin Fluid Layers Undergoing End-Compression. Journal of Fluids Engineering-Transactions of the ASME, 1984. 106(1): pp. 74-78.

[19] Bejan, A., Buckling Flows: A New Frontier in Fluid Mechanics. Annu Rev Numer Fluid Mech Heat Transfer, 1987: pp. 262-304.

[20] Mahadevan, L. And J.B. Keller, Periodic folding of thin sheets (Reprinted from SIAM Journal on Applied Mathematics, vol 55, pg 1609-1624, 1995). Siam Review, 1999. 41(1): pp. 115-131.

[21] Maleki, M., et al., Liquid rope coiling on a solid surface. Physical Review Letters, 2004. 93(21): pp. 4.

[22] Taylor, G.I., Instability of jets, threads, and sheets of viscous fluid, in Proceedings of the 12th International Congress on Applied Mechanics. 1968 Springer, Berlin: Stanford University, Stanford.

[23] Zak, M., Shape instability in thin viscous films and jets. Acta Mechanical, 1985. 55(1): pp. 33-50.

[24] Mahadevan, L., W.S. Ryu, and A.D.T. Samuel, Fluid 'rope trick' investigated. Nature, 2000. 403(6769): pp. 502-502.

[25] Ribe, N.M., Coiling of viscous jets. Proceedings of the Royal Society of London Seri es a-Mathematical Physical and Engineering Sciences, 2004. 460(2051): pp. 3223-3239.

[26] John W. M. Bush and Jeffery M. Aristoff The influence of surface tension on the circular hydraulic jump, J. Fluid Mech. (2003), vol. 489, pp. 229–238.

[27] John W. M. Bush, Jeffery M. Aristoff and A. E. Hosoi An experimental investigation of the stability of the circular hydraulic jump, J. Fluid Mech. (2006), vol. 558, pp. 33–52.

[28] A. R. Teymourtash, M. Passandideh-Fard and M. Khavari, Experimental and Numerical Investigation of Circular Hydraulic Jump, Proceedings of ISME 2010.